Sains Malaysiana 41(7)(2012): 841–846

Application of a Simple Mono Window Land Surface Temperature Algorithm from Landsat ETM+ Over Al Qassim, Saudi Arabia

(Aplikasi Algoritma Tetingkap Mono Suhu Permukaan Tanah Daripada Landsat ETM+ bagi Al QAssim, Saudi Arabia)

H. S. LIM*, M. Z. MAT JAFRI, K. ABDULLAH & SULTAN ALSULTAN

ABSTRACT

This study was conducted to retrieve the land surface temperature (LST) from Landsat ETM+ data for Al Qassim, Saudi Arabia. The proposed technique employed a mono window LST algorithm for retrieving surface temperature from Landsat ETM+. The land surface emissivity and solar angle values were needed in order to apply these in the proposed algorithm. The surface emissivity values were computed based on the NDVI values. The LST values derived from ATCOR2_T in the PCI Geomatica image processing software was used for algorithm calibration. The results showed a high correlation coefficient (R) and low root-mean-square error (RMS) between the LST values retrieved from the proposed algorithm and ATCOR2_T. This study indicated that the proposed algorithm is capable of retrieving accurate LST values and the derived information can be used in the environmental impact assessment for Al Qassim area.

Keywords: Algorithm; ATCOR2_T; LST

ABSTRAK

Kajian ini dilakukan dengan mendapatkan suhu permukaan tanah (LST) daripada data Landsat ETM+ untuk Al Qassim, Arab Saudi. Teknik yang dicadangkan ini menggunakan algoritma tetingkap mono LST untuk mendapatkan suhu permukaan daripada Landsat ETM+. Nilai pancaran permukaan tanah dan nilai-nilai sudut suria diperlukan untuk melaksanakan dalam algoritma yang dicadangkan. Nilai pancaran permukaan tersebut dikira berdasarkan nilai NDVI. Nilai LST berasal daripada ATCOR2_T dalam perisian computer Geomatica PCI digunakan untuk kalibrasi algoritma. Hasilnya menunjukkan pekali korelasi yang tinggi (R) dan nilai sisihan punca min kuasa dua yang rendah (RMS) antara LST nilai dianggarkan daripada algoritma yang dicadangkan dan ATCOR2_T. Kajian ini menunjukkan bahawa algoritma yang dicadangkan mampu mendapatkan nilai LST dengan kejituan yang tingggi dan maklumat yang diperoleh boleh digunakan dalam penilaian kesan persekitaran untuk kawasan Al Qassim.

Kata kunci: Algorima; ATCOR2_T; LST

INTRODUCTION

Land surface temperature (LST) is an important parameter in the field of atmospheric sciences as it combines the result of all surface-atmosphere interaction and energy fluxes between the ground and the atmosphere and is, therefore, a good indicator of the energy balance at the Earth's surface (Wan & Snyder 1996). Many researchers retrieve LST from remotely sensed data (Cristóbal et al. 2009; Jimenez-Munoz & Sobrino 2009; Mallick et al. 2008). LST controls the surface heat and water exchange with atmosphere. The spilt-window technique for retrieving LST from satellite imagery cannot be applied to the Landsat ETM+ image because Landsat ETM+ has one thermal band only.

Direct methods combine *in situ* measurements of temperature and moisture with atmospheric radiative transfer models, such as LOWTRAN and MODTRAN, which calculate the atmospheric transmittance and path radiance as a function of wavelength. Indirect methods derive vertical soundings of the atmosphere from satellite observations and use atmospheric radiative transfer models (Yang & Wang 2002). In the literature, many studies using mono window (Jiménez-Muñoz et al. 2009; Jimenez-Munoz & Sobrino 2009) and split window to retrieve the LST from remotely sensed data (Jimenez-Munoz & Sobrino 2008) has been reported. In this study, we used a single channel algorithm that requires the surface emissivity and incoming solar radiation to retrieve LST over Al Qassim, Saudi Arabia. The objective of this study was to test the single channel algorithm for retrieval of LST from remotely sensed data.

STUDY AREA

The selected study area was centered on the city of Al Khabra in Al Qassim state, which is situated along Wadi Ar Rumah, Saudi Arabia. Figure 1 shows the study area

of the city of Alkhabra and its surrounding desert terrain. The urban transportation network of Buraydah dominates the central portion of the image. Though large portions of the surrounding terrain contain desert features such as sand dunes and Sabkah lakes. The western portion of the city is dominated by Date Palm Grove vegetation and agriculture. There are definitely areas of Buraydah that are clearly being affected by dune encroachment. Our preliminary analysis clearly indicates that satellite imagery and the use of Land Cover Mapping provides a means to identify and quantify the effects of desert processes upon urban areas.

Results and Data Analysis

This study used data recorded from a remote sensing satellite that is owned by NASA of USA – Landsat ETM+. The data was recorded on 20 May 2003 over Al Qassim (Figure 2). The satellite path and row is 168/42. In order to estimate LST from Landsat data, the methodology in this study will be divided into three phases: data calibration, conversion from radiance to brightness temperature, and LST retrieval.

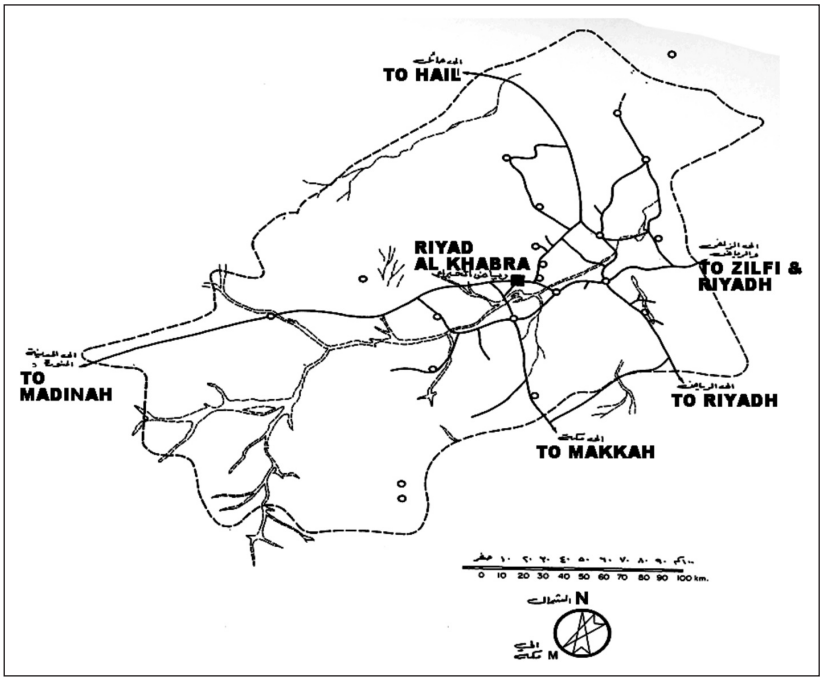

FIGURE 1. The study area of the city of Al Khabra, Saudi Arabia

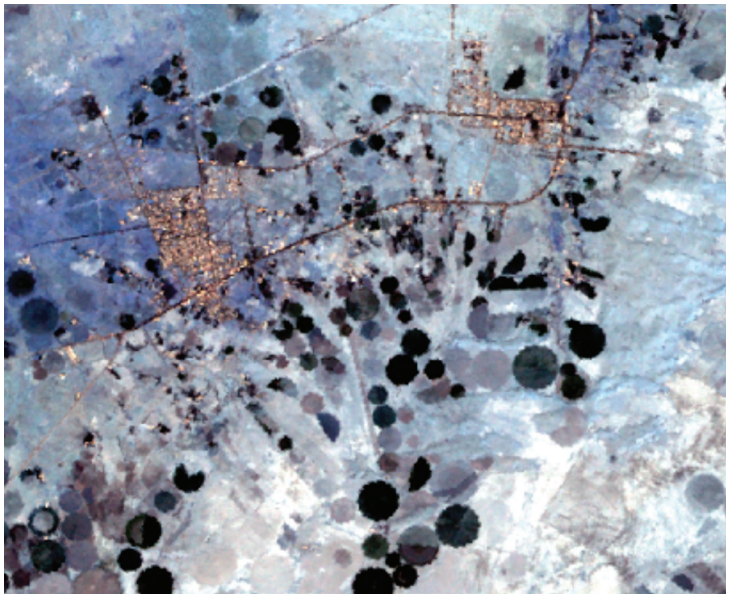

FIGURE 2. Raw satellite image (combination of band 3, 2 and 1)

Usually the problem of non-homogenous in time series of satellite images exists in multi-temporal satellite images. Hence, it affects the analysis of abrupt change in the vegetation cover (Vicente-Serrano et al. 2008). This problem is mainly caused by the absorption and scattering effect from the aerosol particles and gaseous traveling through the Earth and back to the sensor itself. It also caused by the noise from the surface signals. Furthermore, the atmospheric effects may yield error of the obtained result due to misinterpretation of the satellite images (Tokola et al. 1999). Therefore, the sensor calibration should be done when analyzing change detection, especially in normalized difference vegetation index (NDVI).

In radiometric calibration, a precise conversion of the digital number (DN) for Landsat images to satellite radiance unit (L) (Chander et al. 2009b; Vicente-Serrano et al. 2008) is possible by using the following equation:

$$L_\lambda = \left(\frac{LMAX_\lambda - LMIN_\lambda}{Q_{calmax} - Q_{calmin}} \right) \left(Q_{cal} - Q_{calmin} \right) + LMIN_\lambda, \quad (1)$$

where L_λ is the spectral radiance at the sensor's aperture, W $m^{-2}sr^{-1}\mu m^{-1}$, $LMAX_\lambda$ is the spectral radiance scaled to Q_{calmax}, W $m^{-2}sr^{-1}\mu m^{-1}$, $LMIN_\lambda$ is the spectral radiance scaled to Q_{calmin}, W $m^{-2}sr^{-1}\mu m^{-1}$, Q_{calmax} is the maximum quantised calibrated pixel value (DN = 255) corresponding to $LMAX_\lambda$, Q_{calmin} is the minimum quantised calibrated pixel value (DN is the 0 corresponding to $LMIN_\lambda$, Q_{cal} is the quantised calibrated pixel value (DN).

All the related constants were obtained through the study done by Chander et al. (2009a).

The obtained value of radiance was converted to Top of the Atmosphere (TOA) reflectance according to Chander et al. (2009a):

$$\rho = \frac{\pi L d^2}{ESUN_\lambda \cos\theta}, \quad (2)$$

where ρ is the TOA reflectance for band λ, d is the Earth-Sun distance in astronomical units, $ESun_\lambda$ is the mean solar-exoatmospheric irradiance for band λ, and θ is the solar zenith angle in degrees. $ESun_\lambda$ values were obtained from Chander & Markham (2009b) for the ETM+ image or from the Landsat-7 Science Data User Handbook for the ETM+ image. The advantage of TOA reflectance can normalize the sensor due to differing solar zenith angle at the different time and date of satellite images acquisitions. In addition, TOA reflectance also minimized the Earth-Sun distance in multi-temporal.

The value of brightness temperature is required to generate. The assumption made that the at-sensor brightness temperature of the Earth's surface is a black body, includes atmospheric effects. The conversion of the brightness temperature from at-sensor radiance is given by (Chander et al. 2009a, 2009b):

$$T = \frac{K_2}{LN\left[\frac{K_1}{L_\lambda} + 1\right]}, \quad (3)$$

where T is the effective at-sensor brightness temperature (in Kelvin), K_1 is the calibration constant 2 (in Kelvin), K_2 is the calibration constant 1 (W/ (m^2 sr μm)), L_λ is the spectral radiance at the sensor's aperture (W/ (m^2 sr μm)), and LN is the natural logarithm.

Surface emissivity and incoming solar radiation are the required parameters to be used in the proposed algorithm. The solar zenith angle was used to replace the incoming solar radiation in this analysis because they are highly correlated and can be calculated easily (Yang & Wang 2001). The surface emisivity was calculated based on the estimated NDVI values. The emissivity values were obtained from the NDVI as follows:

1. NDVI < 0.2

In this case, the pixel is considered as bare soil and the mean emissivity value used in this study was 0.97 (Sobrino et al. 2004).

2. NDVI>0.5

Pixels with NDVI values higher than 0.5 are considered as fully vegetated, and then a constant value for the emissivity is assumed, typically of 0.99.

3. 0.2<NDVI<0.5

In this case, a mixture of the bare soil and vegetation composes the pixel, and the emissivity is calculated according to the following equation:

$$\varepsilon = \varepsilon_v P_v + \varepsilon_s (1 - P_v) + d\varepsilon, \quad (4)$$

where ε_v is the vegetation emissivity and ε_s is the soil emissivity, P_v is the proportion of vegetation obtained according to (Sobrino et al. 2004):

$$P_v = \left[\frac{NDVI - NDVI_{\min}}{NDVI_{\max} - NDVI_{\min}} \right]^2 \quad (5)$$

$NDVI_{\max} = 0.5$ and $NDVI_{\min} = 0.2$.

The term in (4) includes the effect of the geometrical distribution of the natural surfaces and also the internal reflections. For plain surfaces, this term is negligible, but for heterogeneous and rough surfaces, such as forest, this term can reach a value of 2%. A good approximation for this term can be given by:

$$d\varepsilon = (1 - \varepsilon_s)(1 - P_v) F \varepsilon_v, \quad (6)$$

where F is a shape factor (Sobrino et al. 1990) whose mean value, assuming different geometrical distributions, is 0.55.

Another parameter needed for the algorithm regression was the incoming solar radiation. The solar zenith angles were used as replacement of incoming solar radiation. The proposed model is shown in (7) (Yang & Wang 2002).

$$T_G = a_0 + a_1 T_B^2 + {}_{a2}T_B + a_3\varepsilon + a_4\theta, \quad (7)$$

where T_G is the ground truth temperature, T_B is the brightness temperature, ε is the surface emissivity, θ is the solar angle, a_i is the slgorithm coefficient, i is the 0, 1,2, 3 and 4 are then empirically determined.

A total of 49 locations over Al Qassim, Saudi Arabia were selected randomly and then the LST was calculated using algorithm regression analysis. The results obtained by using mono window are summarized in Table 1. Relative performance between the algorithm that used original satellite brightness temperature and the proposed algorithm which incorporated surface emissivity and solar angle is shown in Table 2. The reference LST values used in the algorithm calibration were derived from ATCOR2_T in the PCI Geomatica image processing software. ATCOR2_T creates a thermal map for a flat area. Many researcher using this PCI Geomatica image processing software to retrieve the LST values (Tan et al. 2009, 2010 and 2011).

In this study, we presented the application of the method of mono-window for retrieving LST. In fact, there are many factors affecting the retrieval of LST from remotely sensed data, but we only considered two variables, surface emissivity and solar incoming radiation in this study. These two parameters have been demonstrated to give a significant effect in the retrieval of LST from satellite thermal data. The algorithm regression results (Table 1) showed that the correlation between the predicted LST and the brightness temperature increased significantly when the proposed model was used. The proposed algorithm produced higher correlation coefficient (R=0.8102) between the predicted LST and the reference LST values computed using ATCOR2_T and lower RMS value (1.0325°C) compared to other algorithm (Table 2).

The determination of coefficient, R, increased from 0.0058 to 0.8102. The RMS value also decreased from 5.2151 °C to 1.0325 °C. This indicates that the Landsat TM/ETM+ thermal infrared data can be calibrated using appropriate ground truth and ancillary data.

Actually, many factors are required in retrieving the LST from satellite data such as transmittance, air moisture, downwelling and upwelling radiance were very difficult to make available for the study. In this study, only two parameters of surface emissivity and incoming solar radiation were used in the model in order to obtain the LST values. The solar zenith angle was used to replace the incoming solar radiation in analysis because they are highly correlated but solar zenith angle can be calculated easily (Cresswell et al. 1999).

The proposed model using surface emissivity and solar angle also had been used in the previous study for the same study area. Yang and Wang (2002) also used

TABLE 1. Data set of 49 locations

	LST derived from ATCOR2_T	Calculated LST
1	28.5	28.25
2	29.5	29.12
3	27.0	26.55
4	26.0	25.65
5	25.5	25.26
6	22.5	21.59
7	28.5	27.59
8	26.5	25.61
9	29.5	28.92
10	22.5	23.25
11	25.0	24.87
12	25.5	24.86
13	29.5	30.22
14	27.5	26.62
15	28.0	27.51
16	26.5	25.25
17	28.5	27.59
18	25.5	24.95
19	26.5	27.01
20	27.5	28.20
21	26.5	27.25
22	23.5	24.15
23	24.0	24.56
24	26.5	27.12
25	25.0	25.62
26	28.5	27.59
27	29.5	28.95
28	25.5	26.21
29	26.5	25.69
30	28.5	28.25
31	26.5	27.25
32	25.5	24.59
33	28.5	28.12
34	25.5	24.90
35	26.0	25.69
36	28.0	27.89
37	29.0	28.56
38	24.5	24.58
39	25.5	25.60
40	24.5	24.58
41	26.5	26.59
42	28.5	28.54
43	26.5	27.12
44	29.5	29.25
45	28.5	28.97
46	27.5	27.59
47	25.5	25.69
48	28.5	27.89
49	28.5	28.58

TABLE 2. Comparative performance of the LST models

Algorithm Models	*R*	RMS (°C)
Model using original satellite brightness temperature	0.0058	5.2151
Model using surface emissivity and solar angle	0.8102	1.0325

TABLE 3. Summary comparative performance of the LST models (with and without added surface emissivity and solar angle) from previous studied

Previous Studied	*R* (with added surface emissivity and solar angle)	*R* (without added surface emissivity and solar angle)
Sultan AlSultan, et al. (2005a)	0.1241	0.7915
Sultan AlSultan, et al. (2005b)	0.1025	0.7921
Lim et al. (2006)	0.3025	0.8352
Lim et al. (2007)	0.4152	0.9256
Sultan AlSultan, et al. (2008)	0.5001	0.8125

this model in their study and this model produced a high accuracies. In their studied, an increasing of *R* value from 0.6 for the model without added surface emissivity and solar angle to 0.9 with added surface emissivity and solar angle. From the previous studied, we also found that this proposed model produced the highest and consistent accuracies (AlSultan et al. 2005). A summary of relative performance between the algorithm that used original satellite brightness temperature and the proposed algorithm which incorporated surface emissivity and solar angle from previous studied are shown in Table 3.

In the future, a more accurate method of surface emissivity estimation can be applied to improve LST retrieved values. This simple model can be applied for accurate computation of LST from Landsat ETM+ data which requires just two parameters such as surface emissivity and solar incoming radiation.

CONCLUSION

The result showed that estimation of land surface temperature using thermal band 6 of Landsat 7 satellite gave a promising result. The algorithm accuracy improved significantly when the surface emissivity and incoming solar radiation was used. The RMS value decreased from 5.2151 K to 1.0325 K using the proposed mono algorithm.

ACKNOWLEDGEMENTS

We would like to thank the technical staff who participated in this project. Thanks are extended to USM for support and encouragement. Special thanks are extended to USGS, USA for providing free satellite image used in this study.

REFERENCES

AlSultan, S., Lim, H.S. MatJafri, M.Z. & Abdullah, K. 2005a. An algorithm for land surface temperature analysis of remote sensing image coverage over AlQassim, Saudi Arabia, *Proceeding of the FIG Working Week 2005 and 8th International Conference for Global Spatial Data Infrastructure (GSDI–8) – From Pharaohs to Geoinformatics, Intercontinental Semiramis*, Cairo, TS 27.10 – Remote Sensing and Photogrammetry, Egypt.

AlSultan, S., Lim, H.S. MatJafri, M.Z. & Abdullah, K. 2005b. Land surface temperature estimation over Palestine and Mediterranean. *Proceeding of the Remote Sensing Arabia–For The Betterment of People*. 1st International Conference on Advanced Remote Sensing for Earth Observation; Systems, Techniques, and Applications (Proceeding in CD), Riyadh, Kingdom of Saudi Arabia.

AlSultan, S., Lim, H.S. MatJafri, M.Z. & Abdullah, K. 2008. Algorithm for Remote Sensing of Land Surface Temperature. *Proceeding of the SPIE Europe Security + Defence*. University of Wales Institute, Cardiff, Wales, United Kingdom. Vol. 7114, Electro-Optical Remote Sensing, Photonic Technologies and Applications II, edited by Gary W. Kamerman, Ove K. Steinvall, Keith L. Lewis, Thomas J. Merlet and Richard C. Hollins, 71140R, Digital Object Identifier: 10.1117/12.800150.

Chander, G., Markham. B.L. & Barsi, J.A. 2009a. Revised landsat-5 thematic mapper radiometric calibration. *IEEE Geosci. Remote Sens. Lett.* 4(3): 490–494.

Chander, G., Markham. B.L. & Helder, D.L. 2009b. Summary of current radiometric calibration coefficients for Landsat MSS, TM, ETM+, and EO-1 ALI sensors. *Remote Sens. Environ.* 113: 893–903.

Cresswell, M.P., Morse, A.P., Thomson, M.C. & Connor. S.J. 1999. Estimating surface air temperature, form Meteosat land surface temperatures, using an empirical solar zenith angle model. *Int. J. Remote Sensing* 20(6): 1125-1132.

Cristobal, J., Jimenez-Munoz, J.C., Sobrino, J.A., Ninyerola, M. & Pons, X. 2009. Improvements in land surface temperature

retrieval from the Landsat series thermal band using water vapor and air temperature, *J. Geophys. Res.* 114: D08103, doi:10.1029/2008JD010616.

Lim, H.S., Mat Jafri, M.Z., Abdullah, K., Daraigan, S.G., Hashim, S.A. & Saleh, N.M. 2006. Land surface temperature estimation from Landsat TM thermal measurement over Penang, *Proceeding of the Young Researcher Conference on Applied Sciences (CAS 2006)*, Subang: Malaysia, 291 - 293.

Lim, H.S., MatJafri, M.Z., Abdullah, K., Saleh, N.M. & AlSultan, S. 2007. Application of Remote Sensing for Land surface temperature retrieval over Mecca, *Proceeding of the SPIE Defense and Security Symposium 2007*. Orlando World Center Marriott Resort and Convention Center, Orlando, Florida, USA, Volume 6541, Thermosense XXIX, edited by Kathryn M. Knettel, Vladimir P. Vavilov and Jonathan J. Miles. DOT: 10.1117/12.719062.

Jimenez-Munoz, J.C. & Sobrino J.A. 2008. Split-Window Coefficients for Land Surface Temperature Retrieval From Low-Resolution Thermal Infrared Sensors. *IEEE Geoscience and Remote Sensing Letters* 5(4): 806-809.

Jimenez-Munoz, J.C. & Sobrino, J.A. 2009. A Single-Channel Algorithm for Land-Surface Temperature Retrieval From ASTER Data. *IEEE Geoscience and Remote Sensing Letters* 7(1): 176-179.

Jiménez-Muñoz, J.C., Cristóbal, J., Sobrino, J.A., Sòria, G., Ninyerola, M. & Pon, X. 2009. Revision of the Single-Channel Algorithm for Land Surface Temperature Retrieval From Landsat Thermal-Infrared Data. *IEEE Transactions on Geoscience and Remote Sensing* 47(1): 339 – 349.

Mallick, Y., Kant, Y. & Bharath, B.D. 2008. Estimation of land surface temperature over Delhi using Landsat-7 ETM+. *The Journal of Indian Geophysical Union* 12(3): 131-140.

Sobrino, J.A., Caselles, V. & Becker, F. 1990. Significance of the remotely sensed thermal infrared measurements obtained over a citrus orchard. *ISPRS Photogrammetric Engineering and Remote Sensing* 44: 343– 354.

Sobrino, J.A., Jimenez-Munoz, J.C., El-Kharraz, J., Gomez, M., Romaguera. M. & Soria, G., 2004. Single-channel and two-channel methods for land surface temperature retrieval from DAIS data and its application to the Barrax site. *International Journal of Remote Sensing* 25(1): 215-230.

Tan, K.C., Lim, H.S., MatJafri, M.Z. & Abdullah, K. 2009. Study on Land Surface Temperature Based on Landsat Image over Penang Island, Malaysia, *Proceeding of the 6th International Conference Computer Graphics, Imaging and Visualization 2009 (CGIV 2009)*, Tianjin, China. 525-529. DOI: 10.1109/CGIV.2009.94.

Tan, K.C., Lim, H.S., MatJafri, M.Z. & Abdullah, K. 2010. Landsat data to evaluate urban expansion and determine land use/land cover changes in Penang Island, Malaysia. *Environmental Earth Sciences* 60(7): 1509–1521.

Tan, K.C., Lim, H.S., Mat Jafri, M.Z. & Abdullah, K. 2011. A comparison of radiometric correction techniques when evaluating the relationship between LST and NDVI in Landsat Imagery, *Environmental Monitoring and Assessment* 184: 3813-3829.

Tokola, T., Lofman, S. & Erkkila, A. 1999. Relative calibration of multitemporal landsat data for forest cover change detection. *Remote Sens. Environ.* 68: 1–11.

Vicente-Serrano, S.M., Perez-Cabello, F. & Lasanta, T. 2008. Assessment of radiometric correction techniques in analyzing vegetation variability and change using time series of Landsat images. *Remote Sens. Environ.* 112: 3916–3934.

Wan, Z. & Snyder, W. 1996. *MODIS Land-surface Temperature Algorithm Theoretical Basis Document (LST ATBD)*, version 3.2.

Yang, J.S. & Wang, Y Q. 2002. Estimation of land surface temperature using Landsat–7 ETM+ thermal infrared and weather station data, *Proceedings of Huangshan International Thermal Infrared Remote Sensing Workshop*, July 14–17 Huangshan, Anhui, P.R.China.

H. S. Lim*, M. Z. Mat Jafri & K. Abdullah
School of Physics
Universiti Sains Malaysia
Minden 11800 Penang
Malaysia

Sultan Alsultan
Remote Sensing Center of Environment Consultant
ISPRS, commission 7 WG VII/7
Middle East Coordinator
Malaz, Al Nurii St., P.O.Box.92038
Riaydh City 11653, Saudi Arabia

*Corresponding author; email: hslim@usm.my

Received: 12 April 2011
Accepted: 21 February 2012